Supplementary information

Hinokitiol-fueled disks form exclusionary zones in the presence of iron

Lara Rae Holstein,[ab] Megan S. Santamore,[a] Asahi Tsukamoto,[a] Masayuki Takeuchi,[ab]

Nobuhiko J. Suematsu,[c] and Atsuro Takai*[ab]

[a] Molecular Design and Function Group, National Institute for Materials Science (NIMS), 1-2-1 Sengen, Tsukuba, Ibaraki 305-0047, Japan

[b] Department of Materials Science and Engineering, Faculty of Pure and Applied Sciences, University of Tsukuba, 1-1-1 Tennodai, Tsukuba, Ibaraki 305-8577, Japan

[c] School of Interdisciplinary Mathematical Sciences; Graduate School of Advanced Mathematical Sciences; Meiji Institute for Advanced Study of Mathematical Sciences (MIMS), Meiji University, 4-21-1, Nakano, Tokyo 164-8525, Japan

Experimental methods

Materials: Unless otherwise noted, all reagents and solvents were purchased from Tokyo Chemical Industry, Sigma-Aldrich, Wako Pure Chemical Industries, and Kanto Chemical and used without further purification. Distilled water was obtained from Kyoei Pharmaceutical and polystyrene-block-polyisoprene-block-polystyrene (**SIS**, 22 wt % styrene) was purchased from Sigma-Aldrich. *N*,*N*'-Bis(3-pentyl)perylenediimide (**PDI**) dye was synthesized according to the literature.[S1] Disks (2 mm diameter, 0.5 mm thickness) composed of hinokitiol (**HT**), **SIS**, and **PDI** as a visualizing dye in 1:4:0.025 weight ratio were prepared according to our previous report.[S2]

Videography and video analysis: The movement of disks was monitored from above using a video camera (EOS Kiss X10, Canon; 30 fps), which was fixed to a copy stand (CS-A4, LPL). Distilled water (10 mL or 20 mL, 3 mm in depth) was added to either a Petri dish (7.5 cm in diameter) or a rectangular glass dish (5 × 20 cm) and placed on a flat light panel (white LED light; A4-500, Trytec) to enhance the contrast. The obtained movie data were analyzed using ImageJ (NIH, USA). The observation of self-driven behavior was conducted at least 5 times using fresh materials, including disks from different batches.

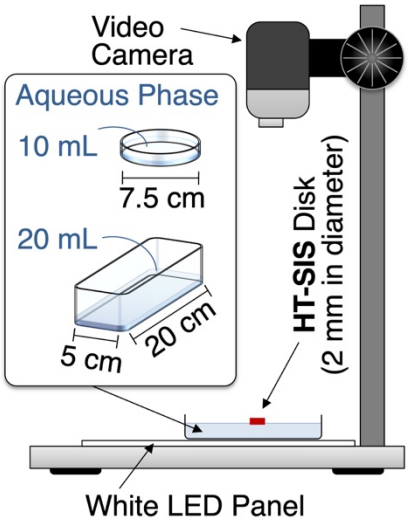

Mass spectrometry: High-resolution mass spectrometry was performed with a Bruker micrOTOF II mass spectrometer, equipped with an atmospheric pressure chemical ionization source (APCI TOF–MS). Isotopic distribution pattern was calculated using an iMass 1.6 software.

Surface tension measurement: The surface tension at solid–water interface was measured by the Wilhelmy method using a DyneMaster DY-300 (Kyowa Interface Science Co., Ltd.). A Pt plate (23.85 mm in the width and 0.15 mm in the thickness) was used as the detector. The amount of each sample in distilled water was varied from 0 to 1.0 mM. In the case of **FeHT$_3$**, 1:3 mixtures of aqueous $FeCl_3$ and **HT** solutions were freshly prepared at the appropriate concentrations and used immediately. Each sample solution (20 mL) was poured into a watch glass (60 mm in diameter) and the surface tension was measured. The surface tension

measurements were performed at least five times, and the average values were plotted against the concentration.

UV-vis absorption spectroscopy: The concentration gradients of $FeCl_3$ and **$FeHT_3$** were estimated by measuring UV-vis absorption spectra recorded on a JASCO V-630 spectrophotometer. Samples (300 µL) were collected using a syringe at various positions from the iron source and placed in a 1 mm quartz cuvette. Due to the propensity of **$FeHT_3$** to accumulate on the aqueous surface, samples were drawn by positioning the tip of the syringe as close to the surface as possible, however there remains some error in the concentration measurements of **$FeHT_3$** due to technical limitations.

Supplementary data

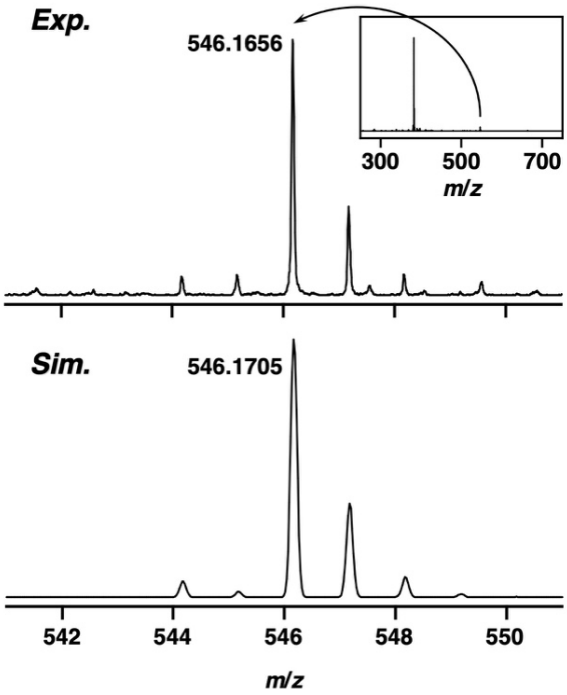

Fig. S1 APCI TOF–MS chart of a 3:1 **HT**:Fe^{III} solution measured in positive ion mode and its calculated isotropic distribution (calcd for $C_{30}H_{33}FeO_6$; $[M+H]^+$). The additional peak at m/z = 382.275 can be attributed to fragmentation ($\mathbf{FeHT_2}^+$) during the ionization process.

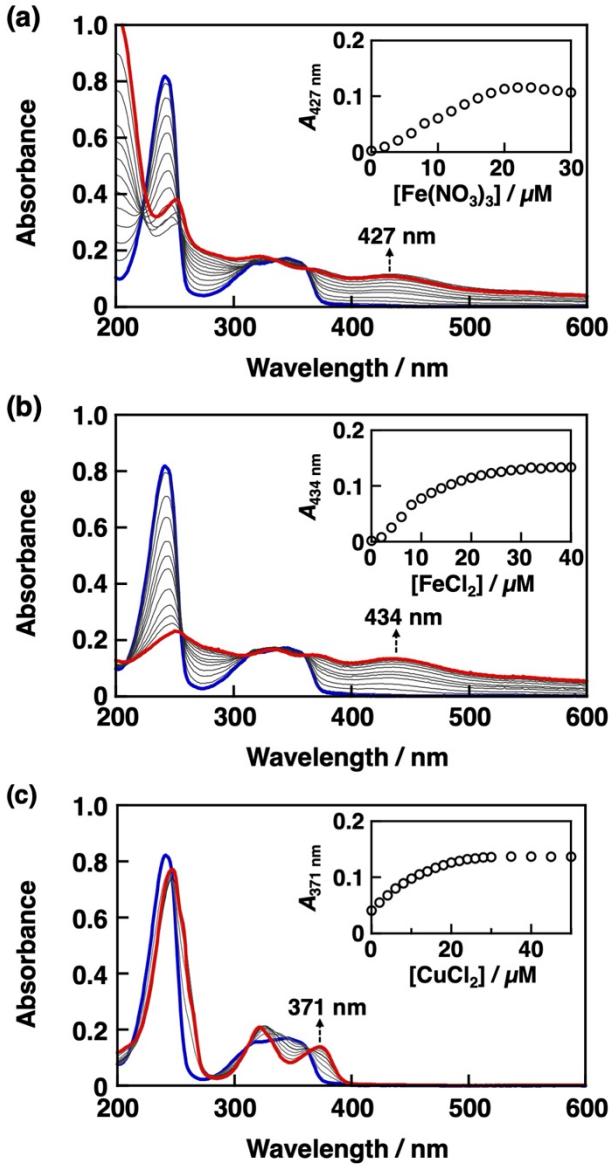

Fig. S2 UV-vis absorption spectral changes of **HT** (30 μM) upon addition of (a) $Fe(NO_3)_3$ (0–30 μM), (b) $FeCl_2$ (0–40 μM), and (c) $CuCl_2$ (0–50 μM) in distilled water at 25 °C. Inset shows the plot of the absorption maximum wavelength of the new absorption band assigned to the metal complex vs. the concentration of metal ion source.

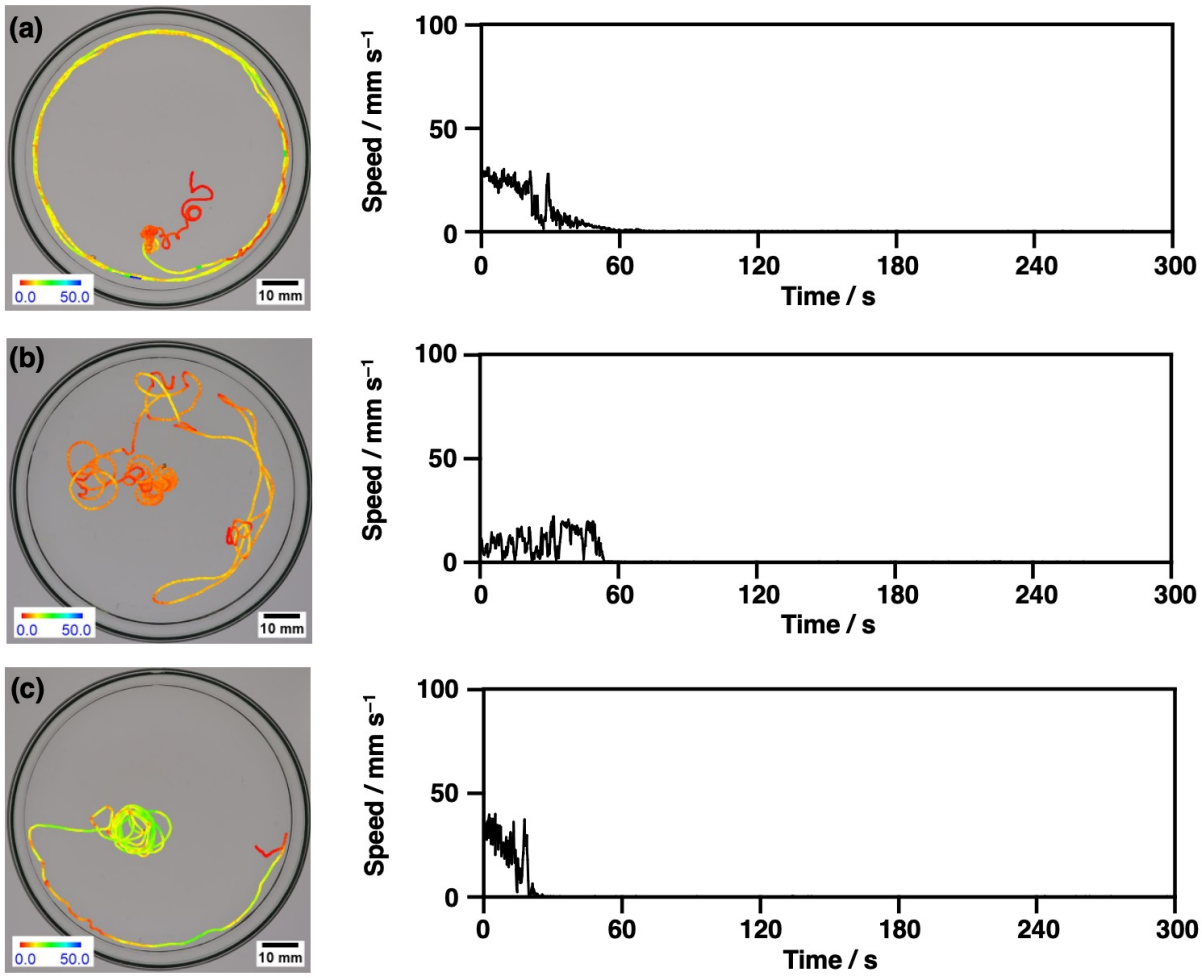

Fig. S3 Trajectory and speed profiles of a pristine **HT** clump placed on (a) 10 μM, (b) 50 μM, and (c) 100 μM aqueous $FeCl_3$ at 25 °C.

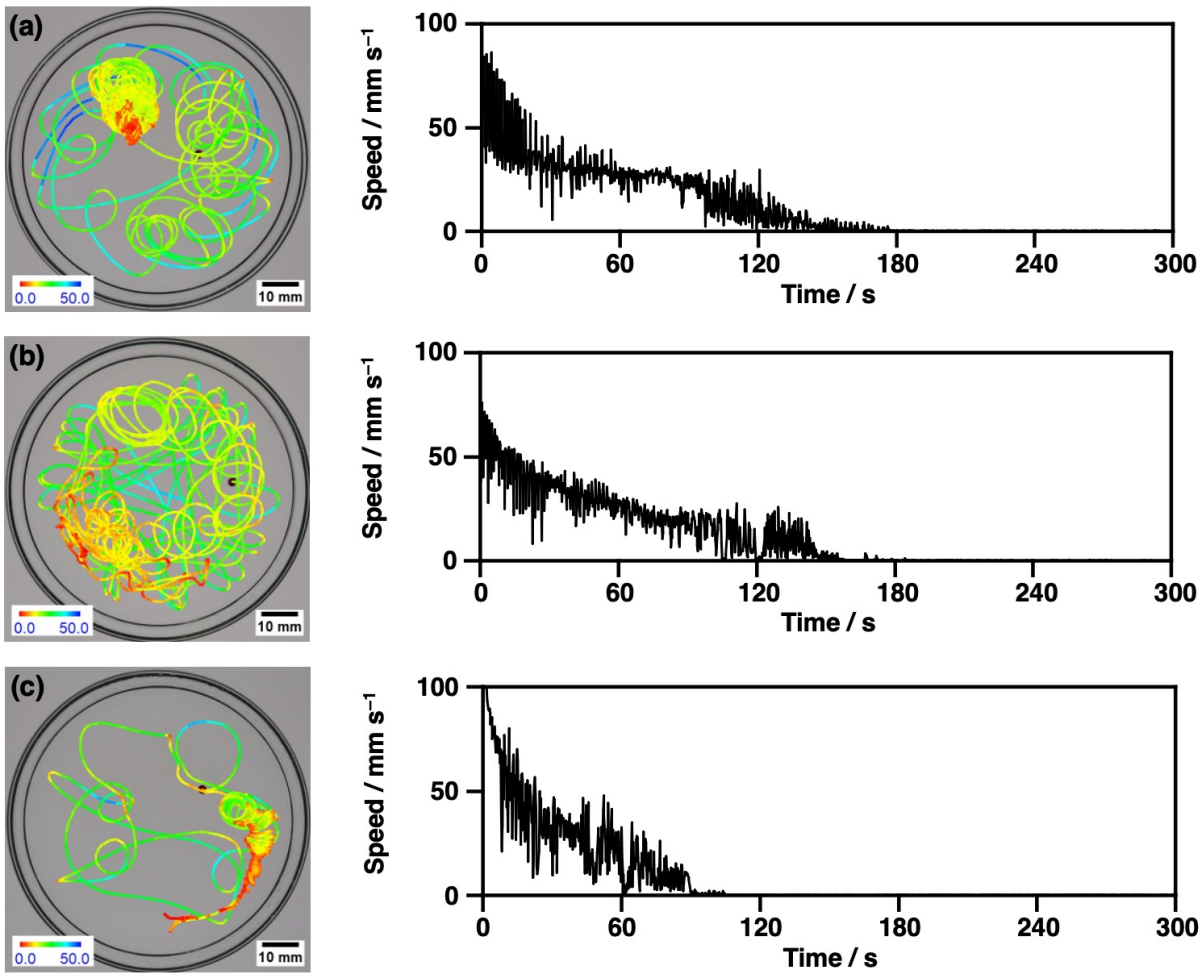

Fig. S4 Trajectory and speed profiles of **HT-SIS** disks when placed on aqueous solutions containing (a) 10 μM, (b) 50 μM, and (c) 100 μM $FeCl_3$ at 25 °C. The color bar represents the average speed (mm s^{-1}) of the disk.

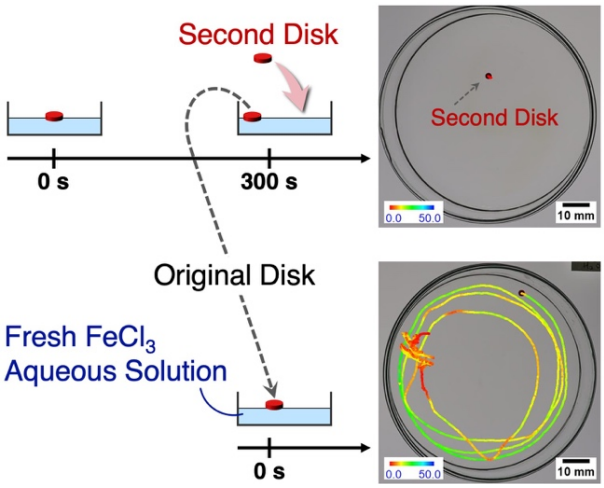

Fig. S5 Schematic illustration (left) and the corresponding trajectory images (right) of a second **HT-SIS** disk (top) placed on aqueous $FeCl_3$ solution after the original disk was allowed to swim for 300 s before it was transferred to fresh $FeCl_3$ solution (bottom). The concentration of ferric iron was set to 100 μM for both solutions.

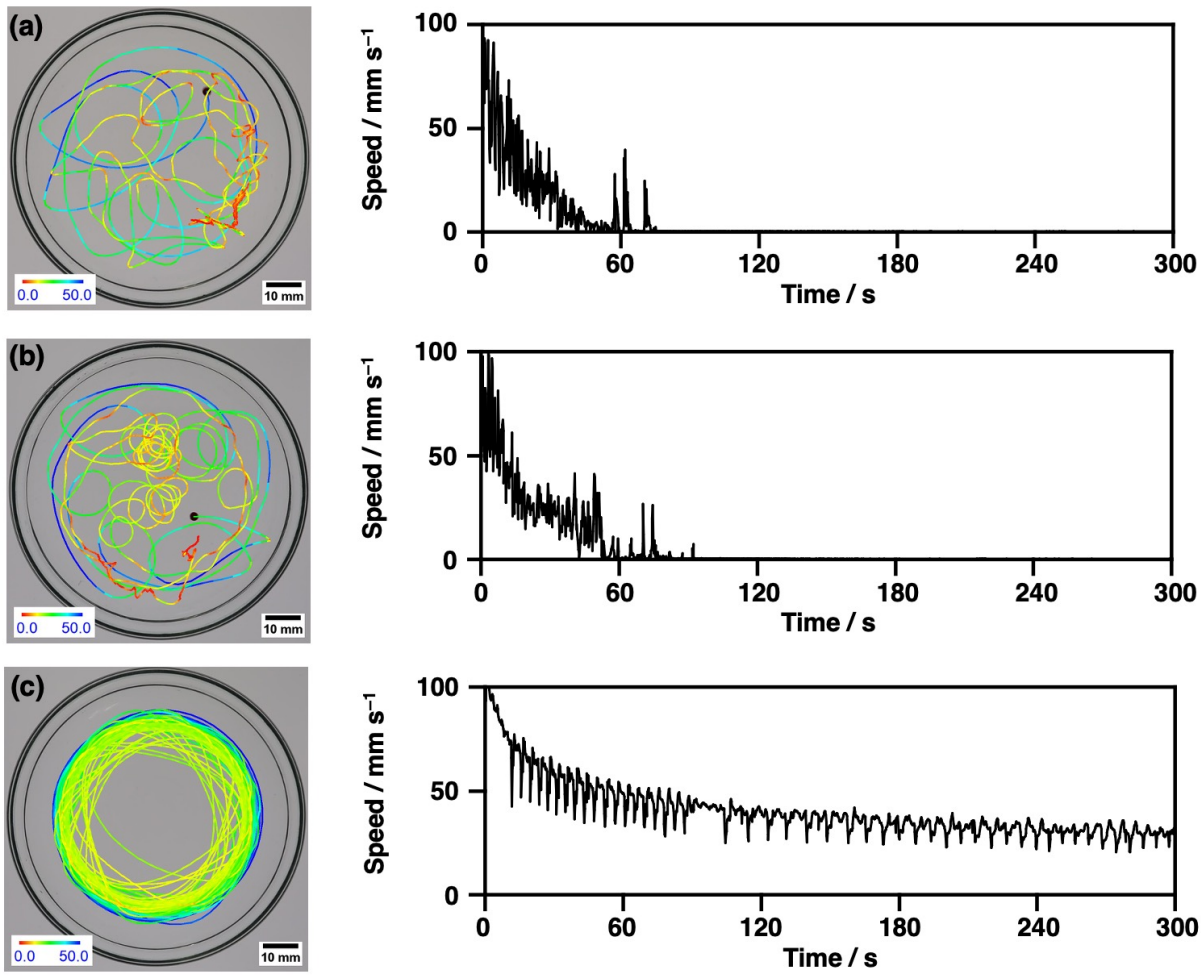

Fig. S6 Trajectory and speed profiles of **HT-SIS** disks when placed on aqueous solutions containing 100 μM (a) $Fe(NO_3)_3$, (b) $FeCl_2$, and (c) $CuCl_2$ at 25 °C. The color bar represents the average speed (mm s^{-1}) of the disk.

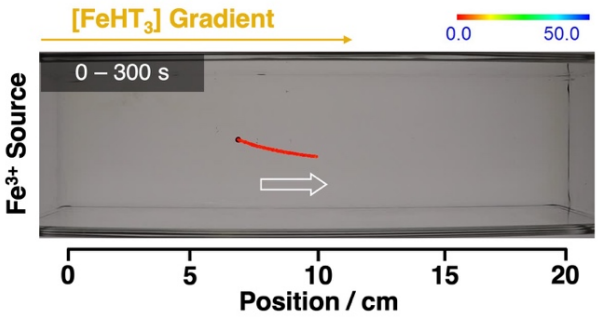

Fig. S7 Trajectory of a **SIS** disk placed at the 7 cm position immediately after removing a **HT-SIS** disk that had been allowed to swim for 600 s at 25 °C. The white arrow indicates the direction of motion.

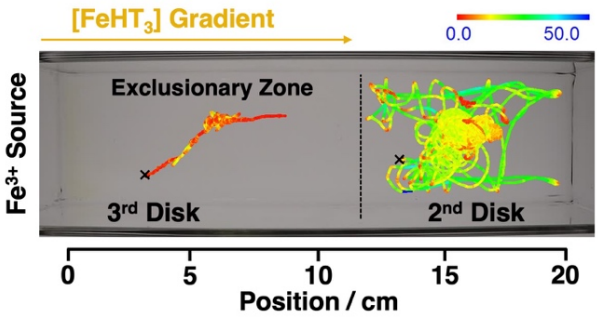

Fig. S8 Trajectories of a second and third **HT-SIS** disk placed on either side of the **$FeHT_3$** barrier formed after the first **HT-SIS** disk was allowed to swim for 600 s at 25 °C. The approximate starting points of the second and third disks are indicated with an x and the boundary of the exclusionary zone is indicated with a black, dashed line. The trajectories were mapped for the first 300 s of motion recorded after the third disk was added.

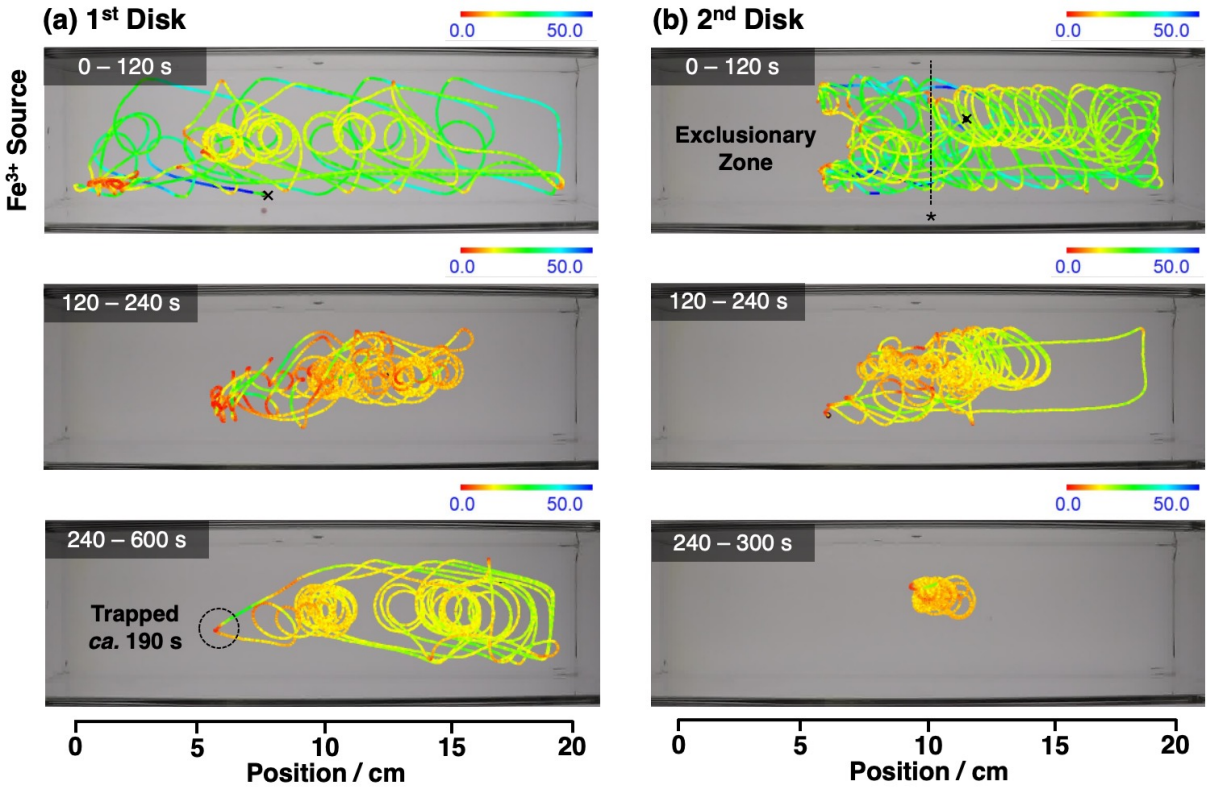

Fig. S9 Trajectory time series of (a) The first **HT-SIS** disk on an Fe^{3+} gradient that did not visit the iron-rich region for long periods of time and (b) a second **HT-SIS** disk in the presence of an **FeHT$_3$** barrier generated by the first disk. The color bar represents the average speed (mm s^{-1}) of the disk and the approximate starting points of the first and second disks are indicated with an x. The black dashed line labeled with an asterisk denotes the position of the barrier in Fig. 3.

Movie legends

Note that all the movies are at 2 × speed.

Supplementary movie 1. Motion of a **HT** clump when floated on a homogeneous aqueous $FeCl_3$ solution (100 μM) at 25 °C.

Supplementary movie 2. Motion of a **HT-SIS** disk when floated on a homogeneous aqueous $FeCl_3$ solution (100 μM) at 25 °C.

Supplementary movie 3. Motion of a **HT-SIS** disk at t = 0–60 s when floated on a Fe^{3+} gradient in distilled water at 25 °C.

Supplementary movie 4. Motion of a **HT-SIS** disk at t = 140–200 s when floated on a Fe^{3+} gradient in distilled water at 25 °C.

Supplementary movie 5. Motion of a **HT-SIS** disk at t = 330–390 s when floated on a Fe^{3+} gradient in distilled water at 25 °C.

Supplementary movie 6. Motion of a second **HT-SIS** disk when floated in the presence of an **$FeHT_3$** exclusionary zone.

Supplementary references

[S1] Y. Yang, Y. Wang, Y. Xie, T. Xiong, Z. Yuan, Y. Zhang, S. Qian and Y. Xiao, *Chem. Commun.* 2011, **47**, 10749.

[S2] L. R. Holstein, M. Takeuchi, N. J. Suematsu and A. Takai, *J. Am. Chem. Soc.* 2025, **147**, 40024.